Two-Tone Signal Generation for Communication Application ADC Testing

Keisuke Kato, Fumitaka Abe, Kazuyuki Wakabayashi, Chuan Gao,
Takafumi Yamada, Haruo Kobayashi, Osamu Kobayashi†, Kiichi Niitsu
Dept. of Electronic Engineering, Gunma University, Kiryu Gunma 376-8515 Japan email: k_haruo@el.gunma-u.ac.jp
† Semiconductor Technology Academic Research Center (STARC), Yokohama 222-0033 Japan

Abstract— **This paper describes algorithms for generating low intermodulation-distortion (IMD) two-tone sinewaves, for communication application ADC testing, using an arbitrary waveform generator (AWG) or a multi-bit ΣΔ DAC inside an SoC. The nonlinearity of the DAC generates distortion components, and we propose here eight methods to precompensate for the IMD using DSP algorithms and produce low-IMD two-tone signals. Theoretical analysis, simulation, and experimental results all demonstrate the effectiveness of our approach.**

Keywords: ADC Testing, Two-Tone Signal, Intermodulation Distortion, Arbitrary Waveform Generator ΣΔ DAC, Digital Pre-Distortion, Distortion Shaping

I. Introduction

Two-tone signal testing is frequently used in ADC testing for communication applications [1], [2], [3]. When the third-order nonlinearity is dominant in a signal generator and two frequency components f_1, f_2 ($f_1 \approx f_2$) are used, the third-order intermodulation distortion (IMD3) components $2f_1 - f_2$, $2f_2 - f_1$ are serious because they are close to the signals (i.e., $2f_1 - f_2$, $2f_2 - f_1 \approx f_1$, f_2) and are difficult to remove with an analog filter.

This paper presents eight algorithms to generate low-IMD two-tone signals using a Nyquist-rate DAC or a (multi-bit) ΣΔ DAC following an analog filter. Their characteristics are as follows:

1) The proposed methods require just the modification of the digital input for the DAC.
2) Exact identification of the DAC nonlinearity is not required.

Since only a relatively low performance DAC is required for the low-IMD two-tone signal generation, our methods can provide low cost testing of communication application ADCs.

Our methods can reduce the IMD close to f_1, f_2 components but produce spurious components far from f_1, f_2 components which are relatively easy to remove with the following analog filter. We call this as distortion shaping which is similar to but different from noise-shaping in a ΣΔ modulator. Our methods are more effective when the DAC sampling frequency goes higher, because the spurious components goes far away from f_1, f_2 [4], [5], [6], [7], [8].

Section II describes four methods using a Nyquist-rate DAC and Section III shows the other four methods using a multi-bit ΣΔ DAC. Section IV provides conclusion.

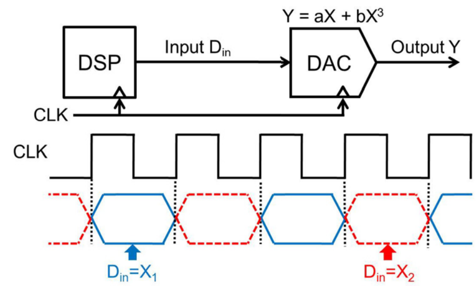

Fig. 1. Proposed method 1, 2 and 3 to generate a low-distortion two-tone signal. DSP provides the input signal X_1 and X_2 alternatively to the following DAC, and distortion components are canceled.

II. Low-IMD Two-Tone Signal Generation with Nyquist-Rate DAC

In this section, we consider to generate a low-IMD two-tone signal with a Nyquist-rate DAC inside an SoC, or using an arbitrary waveform generator (AWG) [4], [5], [7], [8], [9] which consists of DSP (or waveform memory) and a Nyquist-rate DAC.

A. Proposed Algorithm 1: Phase Switching

We use the following two-signal interleaved input for the DAC (Fig.1) [4], [5]:

$$D_{in}(n) = \begin{cases} X_1(n) & \text{in case } n\text{:even} \\ X_2(n) & \text{in case } n\text{:odd.} \end{cases} \quad (1)$$

We denote the sampling period of the DAC as T_s and its sampling frequency as f_s (where $T_s f_s$ =1).
We consider the case that third-order distortion is dominant in the DAC and the even harmonic components are small.

$$Y(nT_s) = a_1 D_{in}(n) + a_3 D_{in}(n)^3. \quad (2)$$

Then we have the following DAC output from eqs.(1),(2):

$$Y(nT_s) = \begin{cases} a_1 X_1(n) + a_3 X_1(n)^3 & \text{in case } n\text{:even} \\ a_1 X_2(n) + a_3 X_2(n)^3 & \text{in case } n\text{:odd.} \end{cases} \quad (3)$$

For a low-IMD3 two-tone signal generation, we propose to use the following:

$$X_1(n) = A\sin(2\pi f_1 nT_s + \frac{\pi}{6}) + B\sin(2\pi f_2 nT_s - \frac{\pi}{6}) \quad (4)$$

$$X_2(n) = A\sin(2\pi f_1 nT_s - \frac{\pi}{6}) + B\sin(2\pi f_2 nT_s + \frac{\pi}{6}). \quad (5)$$

1081-7735/12 $26.00 © 2012 IEEE
DOI 10.1109/ATS.2012.12

IEEE computer society

Then it follows from eqs. (1), (4) and (5) that

$$
\begin{aligned}
Y(nT_s) &= \frac{\sqrt{3}}{2}(a_1 A + \frac{a_3}{4}(3A^3 + 6AB^2))\sin(2\pi f_1 nT_s) \\
&+ \frac{\sqrt{3}}{2}(a_1 B + \frac{a_3}{4}(3B^3 + 6A^2B))\sin(2\pi f_2 nT_s) \\
&- \frac{3\sqrt{3}}{8}a_3 A^2 B \sin(2\pi(2f_1 + f_2)nT_s) \\
&- \frac{3\sqrt{3}}{8}a_3 AB^2 \sin(2\pi(f_1 + 2f_2)nT_s) \\
&+ \frac{1}{2}(a_1 A + \frac{a_3}{4}(3A^3 + 6AB^2))\cos(2\pi(\frac{f_s}{2} - f_1)nT_s) \\
&- \frac{1}{2}(a_1 B + \frac{a_3}{4}(3B^3 + 6A^2B))\cos(2\pi(\frac{f_s}{2} - f_2)nT_s) \\
&- \frac{1}{4}a_3 A^3 \cos(2\pi(\frac{f_s}{2} - 3f_1)nT_s) \\
&+ \frac{1}{4}a_3 B^3 \cos(2\pi(\frac{f_s}{2} - 3f_2)nT_s) \\
&- \frac{3}{8}a_3 A^2 B \cos(2\pi(\frac{f_s}{2} - 2f_1 - f_2)nT_s) \\
&+ \frac{3}{8}a_3 AB^2 \cos(2\pi(\frac{f_s}{2} - f_1 - 2f_2)nT_s) \\
&+ \frac{3}{4}a_3 A^2 B \cos(2\pi(\frac{f_s}{2} - 2f_1 + f_2)nT_s) \\
&- \frac{3}{4}a_3 AB^2 \cos(2\pi(\frac{f_s}{2} + f_1 - 2f_2)nT_s). \qquad (6)
\end{aligned}
$$

We see that the IMD3 ($2f_1 - f_2$, $2f_2 - f_1$) components are canceled in eq.(6).

Numerical simulation results, shown in Fig.2, confirm that the IMD3 components are canceled by the proposed algorithm. Since the high-frequency spurious components in Fig.2 (Right) are far from the signal components f_1, f_2, they are relatively easy to remove by an analog filter after the DAC. Additionally harmonic components have to be removed by the analog filter.

We have performed experiments using an AWG (Agilent 33220A) and a Spectrum Analyzer (ADVANTEST R3267). AWG resolution is 14 bit and sampling rate is 50MHz. Output frequency is f_1 =200kHz and f_2 =220kHz. Fig.3 shows the measurement results and we see that the IMD3 is reduced.

Next we consider also fifth-order nonlinearity as follows:

$$Y(nT_s) = a_1 D_{in}(n) + a_3 D_{in}(n)^3 + a_5 D_{in}(n)^5. \qquad (7)$$

Then we use the four-phase interleave for the DAC input.

$$
D_{in}(n) = \begin{cases} X_1(n) \text{ in case } n = 4k \\ X_2(n) \text{ in case } n = 4k+1 \\ X_3(n) \text{ in case } n = 4k+2 \\ X_4(n) \text{ in case } n = 4k+3. \end{cases} \qquad (8)
$$

Here k is an integer and

$$
\begin{aligned}
X_1(n) &= A\sin(2\pi f_1 nT_s + (4/15)\pi) + B\sin(2\pi f_2 nT_s - (4/15)\pi), \\
X_2(n) &= A\sin(2\pi f_1 nT_s + (1/15)\pi) + B\sin(2\pi f_2 nT_s - (1/15)\pi), \\
X_3(n) &= A\sin(2\pi f_1 nT_s - (1/15)\pi) + B\sin(2\pi f_2 nT_s + (1/15)\pi), \\
X_4(n) &= A\sin(2\pi f_1 nT_s - (4/15)\pi) + B\sin(2\pi f_2 nT_s + (4/15)\pi).
\end{aligned}
$$

Our simulation shows that the IMD3 and IMD5 components are canceled and this is valid even if we change the order of $X_1(n)$, $X_2(n)$, $X_3(n)$ and $X_4(n)$.

The algorithm can be extended to consideration of seventh-order nonlinearity with eight-phase interleave (we have checked by simulation) and so on.

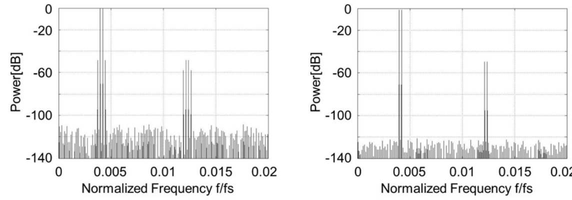

Fig. 2. Simulation results of output power spectrum of a Nyquist-rate DAC with third-order nonlinearity for two-tone input f_1, f_2. (Left) Conventional method. (Right) Proposed method 1.

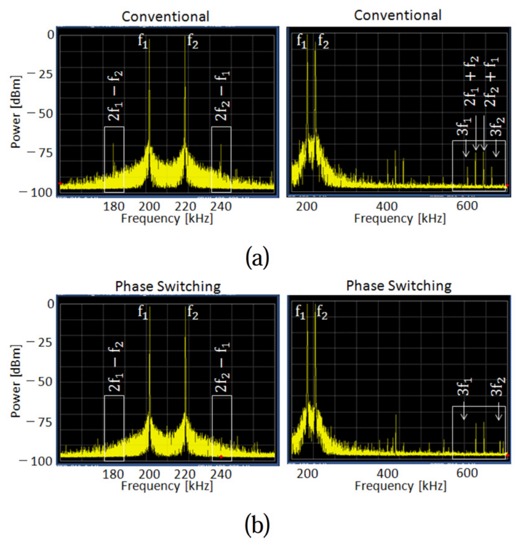

Fig. 3. Experimental results of AWG output power spectrum. (a) Conventional method. (b) Proposed method 1.

B. Proposed Algorithm 2 : Frequency Switching

Next we describe the frequency switching algorithm. Let us use the following X_1 and X_2 for the two-phase interleave in eq.(1):

$$X_1(n) = A\sin(2\pi f_1 nT_s), \quad X_2(n) = B\sin(2\pi f_2 nT_s). \qquad (9)$$

Then it follows from eqs.(2) and (9) that

$$
\begin{aligned}
Y(nT_s) &= (\frac{1}{2}a_1 A + \frac{3}{8}a_3 A^3)\sin(2\pi f_1 nT_s) \\
&+ (\frac{1}{2}a_1 B + \frac{3}{8}a_3 B^3)\sin(2\pi f_2 nT_s) \\
&- \frac{1}{8}a_3 A^3 \sin(2\pi(3f_1)nT_s) \\
&- \frac{1}{8}a_3 B^3 \sin(2\pi(3f_2)nT_s) \\
&+ (\frac{1}{2}a_1 A + \frac{3}{8}a_3 A^3)\cos(2\pi(\frac{f_s}{2} - f_1)nT_s) \\
&+ (\frac{1}{2}a_1 B + \frac{3}{8}a_3 B^3)\cos(2\pi(\frac{f_s}{2} - f_2)nT_s) \\
&- \frac{1}{8}a_3 A^3 \cos(2\pi(\frac{f_s}{2} - 3f_1)nT_s) \\
&- \frac{1}{8}a_3 B^3 \cos(2\pi(\frac{f_s}{2} - 3f_2)nT_s). \qquad (10)
\end{aligned}
$$

Our numerical simulations as well as theoretical analysis show that all of the IMD components (such as IMD3, IMD5, IMD7,

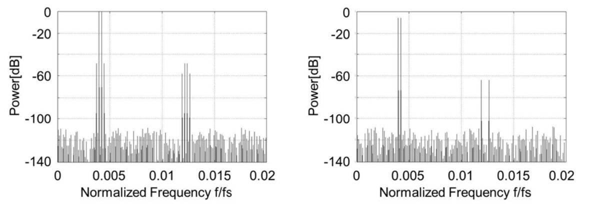

Fig. 4. Simulation results of output power spectrum of a Nyquist-rate DAC with third-order nonlinearity for two-tone input f_1, f_2. (Left) Conventional method. (Right) Proposed method 2.

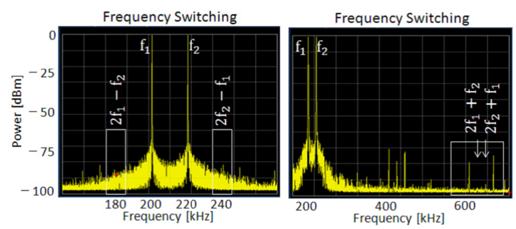

Fig. 5. Experimental results of AWG output power spectrum wih the proposed method 2.

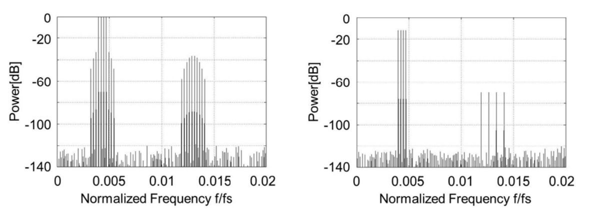

Fig. 6. Simulation results of output power spectrum of a Nyquist-rate DAC with third-order nonlinearity for two-tone input f_1, f_2, f_3 and f_4. (Left) Conventional method. (Right) Proposed method 2.

...) are canceled (Fig.4).

Fig.5 shows the measurement results and we see that IMD3 components are reduced.

This algorithm can be extended to the multi-tone signal generation. For example, let us use the following X_1, X_2, X_3 and X_4 for the four-tone signal with the four-phase interleave in eq.(8):

$$X_1(n) = A_1 \sin(2\pi f_1 n T_s), \quad X_2(n) = A_2 \sin(2\pi f_2 n T_s),$$
$$X_3(n) = A_3 \sin(2\pi f_3 n T_s), \quad X_4(n) = A_4 \sin(2\pi f_4 n T_s).$$

Our simulation shows that f_1, f_2, f_3 and f_4 components are generated without IMD components (Fig.6).

C. Proposed Algorithm 3 : Combination of Phase and Frequency Switching

Next we describe here an algorithm with combination of phase and frequency switchings, which uses the following four-phase interleave input signal:

$$X_1(n) = A \sin(2\pi f_1 n T_s - \frac{\pi}{6}), \quad X_2(n) = B \sin(2\pi f_2 n T_s + \frac{\pi}{6}),$$
$$X_3(n) = A \sin(2\pi f_1 n T_s + \frac{\pi}{6}), \quad X_4(n) = B \sin(2\pi f_2 n T_s - \frac{\pi}{6}).$$

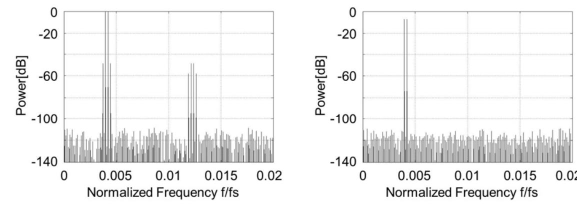

Fig. 7. Simulation results of output power spectrum of a Nyquist-rate DAC with third-order nonlinearity for two-tone input f_1, f_2. (Left) Conventional method. (Right) Proposed method 3.

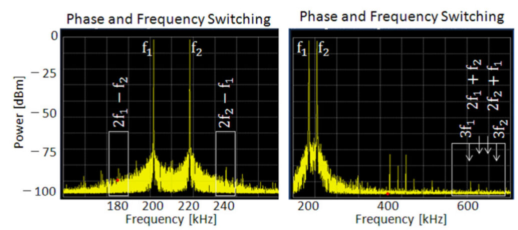

Fig. 8. Experimental results of AWG output power spectrum with the proposed method 3.

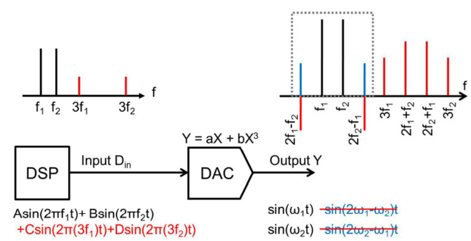

Fig. 9. Principle of the proposed method 4.

This method can cancel HD3 as well as IMD3, and Fig.7 shows the simulation results. Fig.8 shows the measurement results and we see that IMD3 and HD3 components are reduced.

Fig.12 shows the measurement result comparison of the conventional and proposed methods 1, 2, & 3.

D. Proposed Algorithm 4 : Pre-Distortion

We describe another precompensation method for the IMD3 components using a DSP algorithm by adding $3f_1$, $3f_2$ components at the input (Fig.9): this concept is similar to the predistortion method in power amplifiers [10].

Suppose that the DAC in the AWG has third-order nonlinearity (eq.(2)). Then we propose to use the following $D_{in}(n)$:

$$\begin{aligned} D_{in}(n) &= A \sin(2\pi f_1 n T_s) + B \sin(2\pi f_2 n T_s) \\ &+ C \sin(2\pi (3f_1) n T_s) + D \sin(2\pi (3f_2) n T_s). \end{aligned} \tag{11}$$

Here we set

$$C = A/2. \quad D = B/2. \tag{12}$$

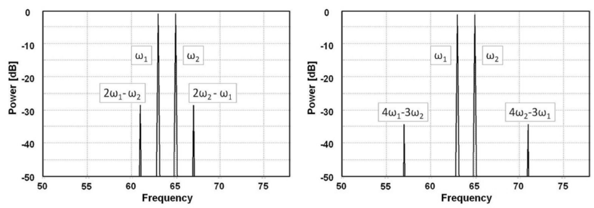

Fig. 10. Simulation results of output power spectrum of a Nyquist-rate DAC with third-order nonlinearity for two-tone input f_1, f_2. (Left) Conventional method. (Right) Proposed method 4.

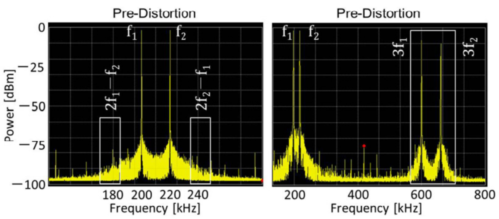

Fig. 11. Experimental results of AWG output power spectrum with the proposed method 4.

By manipulating the above equations, we have V_{out} with f_1, f_2 components and without IMD3 components. V_{out} has other frequency components ($3f_1 - 2f_2$, $3f_2 - 2f_1$) which go far from f_1, f_2 (Figs.9, 10).

Fig.11 shows the spectrum of the AWG outputs with the conventional and proposed methods. Table.I shows the effect of proposed methods. Fig.12 shows experimental result comparison of the conventional and proposed methods. We see that IMD3 suppression is substantial with our methods.

We close this section by remarking that $3f_1-2f_2$, $3f_2-2f_1$ components can be moved to $4f_1 - 3f_2$, $4f_2 - 3f_1$ by adding $5f_1$, $5f_2$ components as well as $3f_1$, $3f_2$ ones at the input, and this can be generalized [8].

TABLE I
EXPERIMENTAL RESULT DIFFERENCE BETWEEN CONVENTIONAL METHOD AND PROPOSED METHODS.

	Fundamental [dB]	IMD3 [dB]	SFDR [dB]
Phase Switching	-1.26	-13.7	12.5
Frequency Switching	-0.01	-10.6	10.6
Phase& Frequency Switching	-1.21	-13.6	12.4
Pre-Distortion	-0.60	11.1	10.5

III. Proposed Algorithm using ΣΔDAC

In this section, we consider to generate a low-IMD two-tone signal with a multi-bit ΣΔ DAC. We apply the proposed algorithms 1, 2, 3 and 4 in the Nyquist-rate DAC case to the multi-bit ΣΔ DAC case (Fig.13) which correspond to the algorithms 5, 6, 7 and 8, respectively. We show with

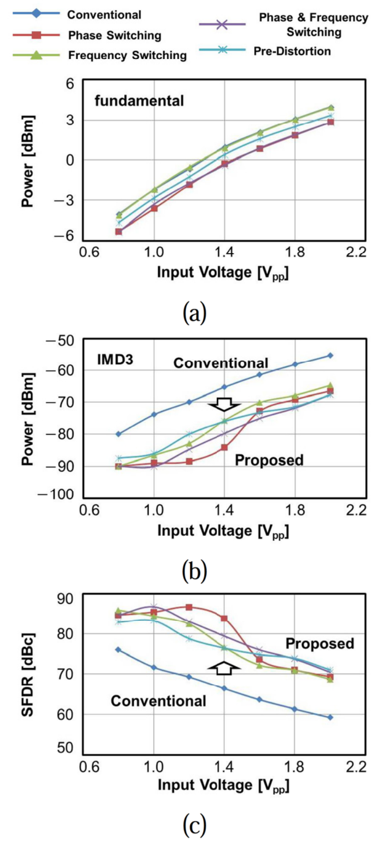

Fig. 12. Experimental result comparison of the conventional, and proposed methods 1, 2 & 3. (a) Fundamental signal power. (b) IMD3. (c) SFDR.

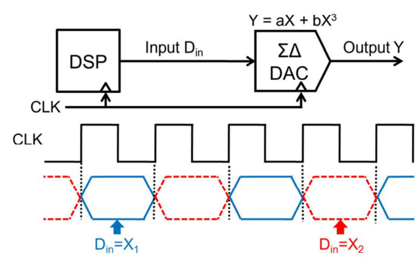

Fig. 13. Proposed methods 5, 6 & 7 to generate a low-distortion two-tone signal with ΣΔ DAC. DSP provides the input signal X1 and X2 alternatively to the following ΣΔ DAC, and distortion components are canceled.

simulations and experiments that all work well, although the analytical proofs may be difficult in ΣΔ DAC case.

Our proposed methods may be implemented by utilizing existing DSP and DAC cores inside an SoC in test mode.

Methods such as dynamic element matching and self-calibration have been used for reducing the effects of multi-bit DAC nonlinearity in ΣΔ modulators [11], but these methods require additional hardware. However, our proposed methods need only a DSP program algorithm change.

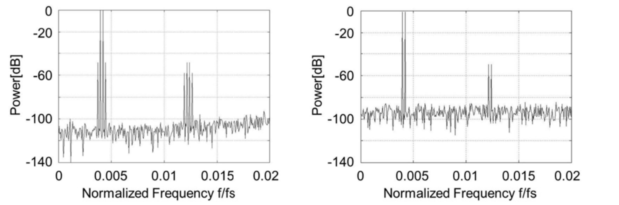

Fig. 14. Simulation results of output power spectrum of a ΣΔ DAC with third-order nonlinearity for two-tone input f_1, f_2. (Left) Conventional method. (Right) Proposed method 5.

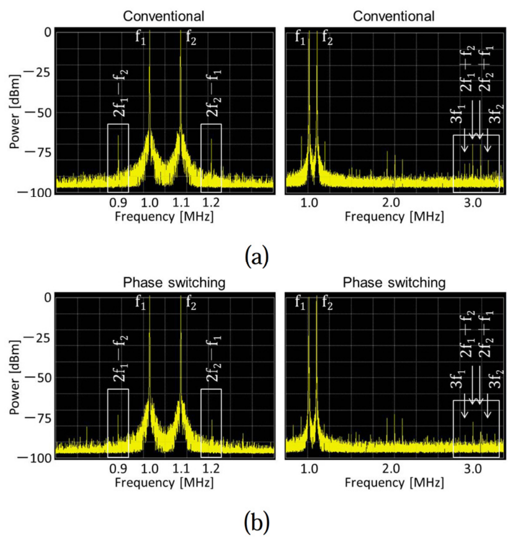

Fig. 15. Experimental results of AWG output power spectrum with a ΣΔ DAC. (a) Conventional method. (b) Proposed method 5.

A. Proposed Algorithm 5 : Phase Switching

We apply the proposed algorithm 1 to the multi-bit ΣΔ DAC [6] for low-IMD two-tone signal generation and we use eqs.(4) and (5). Fig.14 shows simulation results while Fig.15 shows experimental results for two-tone signal generation(f_1 =1.0MHz , f_2 =1.1MHz) using a second-order ΣΔ DAC with 7-bit internal DAC: we see that the proposed algorithm reduces IMD3 components.

B. Proposed Algorithm 6 : Frequency Switching

We apply the proposed algorithm 2 to the multi-bit ΣΔ DAC for low-IMD two-tone signal generation. Fig.16 shows its simulation results while Fig.17 shows experimental results, and we see that IMD3 components are canceled.

C. Proposed Algorithm 7 : Combination of Phase and Frequency Switching

We apply the proposed algorithm 3 to the multi-bit ΣΔ DAC for low-IMD two-tone signal generation. Fig.18 shows its simulation results while Fig.19 shows experimental results, and we see that IMD3 and HD3 components are canceled.

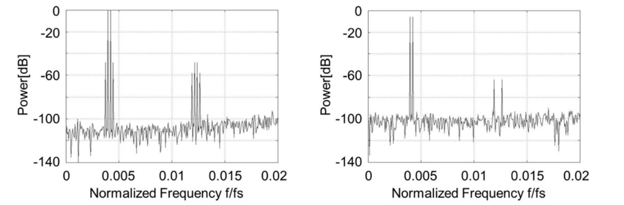

Fig. 16. Simulation results of output power spectrum of a ΣΔ DAC with third-order nonlinearity for two-tone input f_1, f_2. (Left) Conventional method. (Right) Proposed method 6.

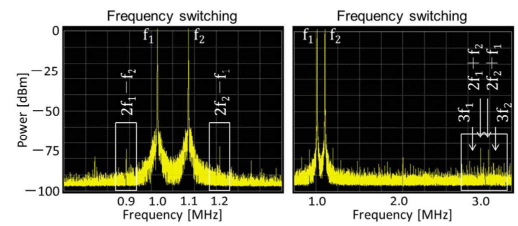

Fig. 17. Experimental results of AWG output power spectrum with a ΣΔ DAC with the proposed method 6.

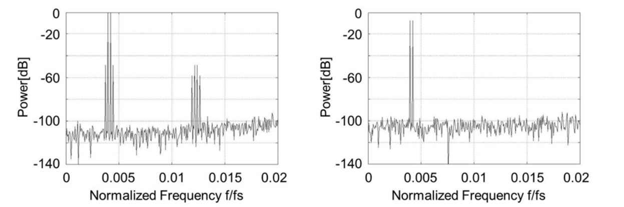

Fig. 18. Simulation results of output power spectrum of a ΣΔ DAC with third-order nonlinearity for two-tone input f_1, f_2. (Left) Conventional method. (Right) Proposed method 7.

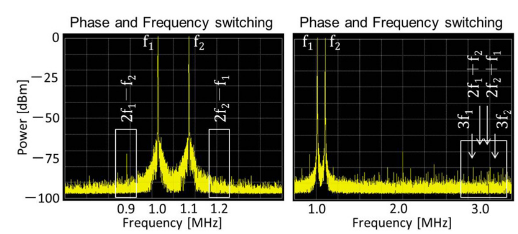

Fig. 19. Experimental results of AWG output power spectrum with a ΣΔ DAC with the proposed method 7.

D. Proposed Algorithm 8 : Pre-Distortion

We apply the proposed algorithm 4 to the multi-bit ΣΔ DAC for low-IMD two-tone signal generation (Fig.20). Fig.21 shows its simulation results while Fig.22 shows experimental results. We see that IMD3 components go away from the signals f_1, f_2.

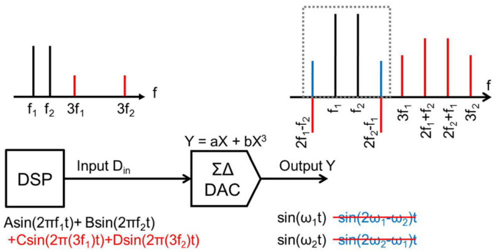

Fig. 20. Principle of the proposed method 8.

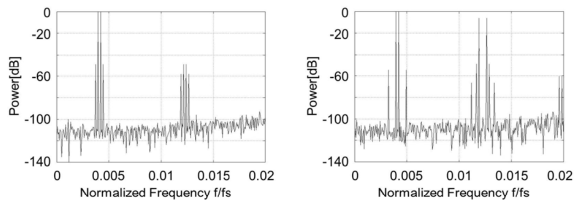

Fig. 21. Simulation results of output power spectrum of a ΣΔ DAC with third-order nonlinearity for two-tone input f_1, f_2. (Left) Conventional method. (Right) Proposed method 8.

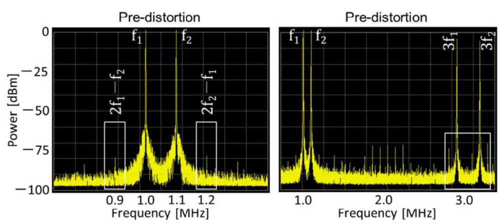

Fig. 22. Experimental results of AWG output power spectrum with a ΣΔ DAC with the proposed method 8.

IV. Concluding Remarks

We have proposed eight algorithms for generating low-IMD two-tone sinewaves, for testing communication application ADCs, using an arbitrary waveform generator (AWG) or a multi-bit ΣΔ DAC inside an SoC. Theoretical analysis, simulation, and experimental results verified the effectiveness of our approach.

All of our methods do not need the DAC nonlinearity identification, and we need only DSP program (or waveform memory contents) change. Our methods become more effective as the DAC frequency goes high, but do not require the DAC linearity, which meets the semiconductor device advancement trends.

Table II shows the comparison of the conventional and proposed methods when the third-order nonlinearity is dominant: there, "cancel" means the canceled spurious or harmonic components and "appear" means the spurious components caused by the corresponding method. Further investigation for merits and demerits of each algorithm, in the view points of signal frequency, IMD reduction, analog filter requirements and DAC sampling speed & resolution is underway.

Finally we remark that the proposed techniques in this paper are to apply for conventional DACs, however we have also exploited a new DAC architecture in [12] to reduce the IMD3 components for the two-tone signal generation for next generation AWGs.

TABLE II
OUTPUT POWER SPECTRUM COMPARISON

	Cancel	Appear
Conventional		$2f_1 - f_2$, $2f_2 - f_1$
Phase Switching	$2f_1 - f_2$, $2f_2 - f_1$ $3f_1$, $3f_2$	around $f_s/2$
Frequency Switching	$2f_1 - f_2$, $2f_2 - f_1$ $2f_1 + f_2$, $2f_2 + f_1$	around $f_s/2$
Phase & Frequency Switching	$2f_1 - f_2$, $2f_2 - f_1$ $2f_1 + f_2$, $2f_2 + f_1$ $3f_1$, $3f_2$	around $f_s/4$, $f_s/2$
Pre-Distortion	$2f_1 - f_2$, $2f_2 - f_1$	$4f_1 - 3f_2$, $4f_2 - 3f_1$ around $3f_1$, $5f_1$, $7f_1$, $9f_1$

Acknowledgment

We acknowledge Y. Yano, T. Gake, N. Takai, T. Matsuura, T. J. Yamaguchi, H. Okawara, H. Sakayori and K. Wilkinson.

References

[1] Y. Motoki, H. Sugawara, H. Kobayashi, T. Komuro, and H. Sakayori, "Multi-Tone Curve Fitting Algorithms for Communication Application ADC Testing", Electronics and Communication in Japan: Part 2, Wiley Periodicals Inc., vol.86, no.8, pp.1-11 (2003).

[2] M. Gustavsson, J. J. Wikner, N. N. Tan. CMOS Data Converters for Communications. Kluwer Academic Publisher (2000).

[3] B. Razavi, RF Microelectronics, Prentice Hall (1998).

[4] K. Wakabayashi, T. Yamada, S. Uemori, O. Kobayashi, K. Kato, H. Kobayashi, K. Niitsu, H. Miyashita, S. Kishigami, K. Rikino, Y. Yano, T. Gake, "Low-Distortion Single-Tone and Two-Tone Sinewave Generation Algorithms Using an Arbitrary Waveform Generator", IEEE International Mixed-Signals, Sensors and Systems Test Workshop, Santa Barbara, CA (May 2011).

[5] K. Wakabayashi, K. Kato, T. Yamada, O. Kobayashi, H. Kobayashi, F. Abe, K. Niitsu, "Low-Distortion Sinewave Generation Method Using Arbitrary Waveform Generator", Journal of Electronic Testing: Theory and Applications, Special Issue on Analog, Mixed-Signal, RF and MEMS Testing vol.28, no.2 (April 2012).

[6] T. Yamada, O. Kobayashi, K. Kato, K. Wakabayashi, H. Kobayashi,T. Matsuura, Y. Yano, T. Gake, K. Niitsu, N. Takai, T. J. Yamaguchi, "Low-Distortion Single-Tone and Two-Tone Sinewave Generation Using ΣΔ DAC", IEEE International Test Conference (poster session), Anaheim, CA (Sept. 2011).

[7] K. Kato, F. Abe, K. Wakabayashi, T. Yamada, H. Kobayashi, O. Kobayashi, K. Niitsu "Low-IMD Two-Tone Signal Generation for ADC Testing", IEEE International Mixed-Signals, Sensors, and Systems Test Workshop, Taipei, Taiwan (May 2012).

[8] K. Kato, K. Wakabayashi, T. Yamada, H. Kobayashi, O. Kobayashi, K. Niitsu, "Low-Distortion Two-Tone Signal Generation with AWG", IEICE Workshop on Circuits and Systems, Awaji-Shima, Japan (Aug. 2012).

[9] A. Maeda, " A Method to Generate a Very Low Distortion, High Frequency Sine Waveform Using an AWG", IEEE International Test Conference (Oct. 2008).

[10] S. C. Cripps, Advanced Techniques in RF Power Amplifier Design, pp.153-195, Artec House (2002).

[11] R. Schreier and G. C. Temes, Understand Delta-Sigma Data Converters, IEEE Press (2005).

[12] C. Gao, K. Wakabayashi, K. Kato, F. Abe, H. Kobayashi, O. Kobayashi, T. Matsuura, K. Niitsu, N. Takai, "Digital-to-Analog Converter Architecture for Low Distortion Signal Generation", IEEJ Technical Meeting of Electronic Circuits, ECT-12-20, Yokosuka, Japan (March 2012).